1702 *Biochemistry* **2010,** *49,* 1702–1712
DOI: 10.1021/bi901760d

BIOCHEMISTRY
including biophysical chemistry & molecular biology
Article

Genistein Arrests Cell Cycle Progression of A549 Cells at the G_2/M Phase and Depolymerizes Interphase Microtubules through Binding to a Unique Site of Tubulin†

Sumita Mukherjee,‡ Bipul Ranjan Acharya,‡ Bhabatarak Bhattacharyya,§ and Gopal Chakrabarti*,‡

‡*Department of Biotechnology and Dr. B. C. Guha Centre for Genetic Engineering and Biotechnology, University of Calcutta, 35 Ballygunge Circular Road, Kolkata, WB 700019, India, and* §*Department of Biochemistry, Bose Institute, Kolkata, WB 700054, India*

Received March 20, 2009; Revised Manuscript Received January 15, 2010

ABSTRACT: Genistein (4′,5,7-trihydroxyisoflavone), an isoflavone, is a major constituent of soyfoods. It has potential antiproliferative activity against several tumor types. We have examined the effect of genistein on cellular microtubules as well as its binding with purified tubulin in vitro. Cell viability experiments using human non-small lung epithelium carcinoma cells (A549) indicated that the IC_{50} value for genistein is 72 μM. Flow cytometry experiments demonstrated that genistein arrested cell cycle progression at the G_2/M phase, but mitotic index data showed that genistein did not arrest cell cycle progression at mitosis. Immunofluorescence studies using an anti-α-tubulin antibody demonstrated a significant depolymerization of the interphase microtubules in a dose-dependent manner, and this was confirmed by the Western blot experiment using genistein-treated A549 cells. In vitro polymerization of purified tubulin into microtubules was inhibited by genistein with an IC_{50} value of 87 μM. Genistein binding to tubulin quenched protein tryptophan fluorescence in a time- and concentration-dependent manner. Binding of genistein to tubulin was slow, taking ~45 min for equilibration at 37 °C. The association rate constant was 104.64 ± 20.63 M^{-1} s^{-1} at 37 °C. The stoichiometry of genistein binding to tubulin was nearly 1:1 (molar ratio) with a dissociation constant of 15 μM at 37 °C. It was interesting to note that genistein did not recognize either the colchicine site or the vinblastine binding site of tubulin. Surprisingly, genistein inhibited ANS binding and competed for its binding site of tubulin with a K_i of 20 μM as determined from a modified Dixon plot. Hence, we conclude that one of the mechanisms of antiproliferative activity of genistein is depolymerization of microtubules through binding of tubulin.

Natural compounds flavonoids and isoflavonoids are currently of great interest because of their antioxidative and anticancer properties (*1*−*6*). Genistein (4′,5,7-trihydroxyisoflavone) (Figure 1) is an isoflavone, mostly present in soybeans, and legumes such as chickpeas contain small amounts of genistein. The compound has multiple functions (*7*−*10*), including G_2/M cell cycle arrest (*8*, *9*). Genistein inhibits tumor formation in animal models of breast (*11*, *12*), prostate (*13*), and bladder cancer (*14*). Genistein is in phase II clinical trial (*15*) and induces apoptosis of lung cancer cells (*16*), breast cancer cells (*17*), bladder cancer cells (*14*), and human prostate cancer cells (*13*). Several mechanisms have been proposed to explain the anticarcinogenic and proapoptotic effects of genistein. Genistein is a phytoestrogen, which binds to the estrogen receptor, and thereby prevents the binding of estrogen for the initiation of cancer growth (*18*). It also resists postmenopausal syndrome, acting as an agonist of estrogen. Genistein is an inhibitor of protein tyrosine kinases (*19*), topoisomerase II (*20*), and angiogenesis (*14*). Proapoptotic factors such as Bax and p21WAF1/CIP1 are induced by genistein in breast cancer cells (*18*) and in prostate cancer cells (*21*). Furthermore, antiapoptotic factor Bcl-2 is inhibited by genistein in breast cancer cells (*9*).

Several flavonoids were reported to exert their antiproliferative activity by targeting microtubules through tubulin binding (*22*). Although the antiproliferative activity of genistein has been reported (*11*−*17*), its relation with tubulin and microtubules has not been studied. Microtubules are polymers of tubulin heterodimers (α- and β-tubulin) that are involved in many cellular functions such as spindle formation, mitosis, cell motility, cell shape, and transportation of various organelles (*23*). The equilibrium between tubulin and microtubules is dynamic in nature, and this dynamicity plays a critical role during spindle formation and chromosome segregation during cell division (*23*). As tubulin and microtubules are involved in cell division, many antimitotic drugs have been targeted to them for the development of anticancer drugs. A large number of compounds, many of which are from natural products, inhibit cell division at the G_2/M phase by perturbing microtubule dynamics (*22*, *24*).

In this study, we show that genistein interacts with tubulin and microtubules in cells as well as purified tubulin in vitro. We demonstrate that genistein arrests cell cycle progression of human non-small lung epithelium cancer (A549) cells at the G_2/M phase and depolymerizes the microtubule network in A549 cells. In vitro, genistein inhibits tubulin polymerization in a concentration-dependent manner. Our results suggest a novel mechanism of action for the inhibition of cell proliferation activity of natural isoflavonoid genistein through binding to tubulin.

†The work was supported by grants from CSIR, Government of India [37(1216)/05/EMR-II], and BRNS/DAE, Government of India (2006/37/21/BRNS), to G.C. S.M. is supported by a fellowship from CSIR, Government of India [Grant 37(1216)/05/EMR-II].

*To whom correspondence should be addressed: Department of Biotechnology and Dr. B. C. Guha Centre for Genetic Engineering and Biotechnology, University of Calcutta, 35 Ballygunge Circular Road, Kolkata, WB 700 019, India. Telephone: 91-33-2461-4983. Fax: 91-33-2461-4849. E-mail: gcbcg@caluniv.ac.in.

 Published on Web 01/19/2010

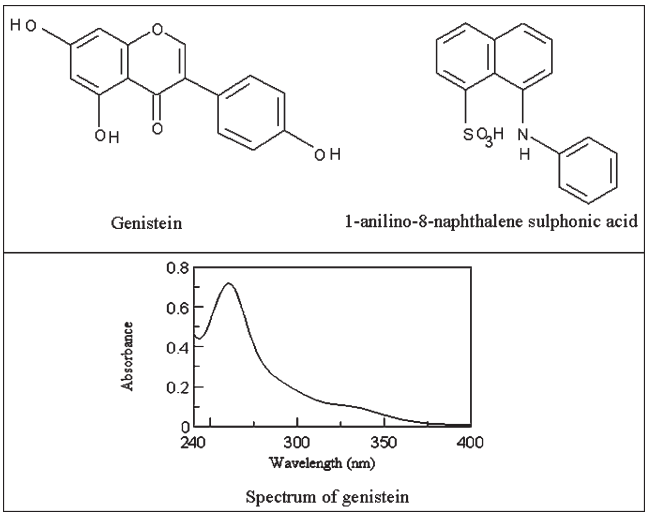

FIGURE 1: Chemical structure of genistein [5,7-dihydroxy-3-(4-hydroxyphenyl)-4*H*-1-benzopyran-4-one, 4′,5,7-trihydroxyisoflavone] and 1,8-ANS (1-anilino-8-naphthalenesulfonic acid). Also shown is the absorption spectrum of 20 μM genistein.

EXPERIMENTAL PROCEDURES

Materials. Genistein, colchicine, PIPES,[1] GTP, EGTA, DTNB, and monoclonal anti-α-tubulin antibody (raised in mouse) were purchased from Sigma. 1-Anilino-8-naphthalenesulfonic acid (ANS) was purchased from Molecular Probes. Nutrient F12 Ham medium (supplemented with 1 mM L-glutamine) and amphotericin B (fungizone) were obtained from Hyclone. Fetal bovine serum and penicillin-streptomycin were obtained from Gibco-Invitrogen. BODIPY-FL-vinblastine (4,4-difluoro-3a,4a-diaza-*s*-indacene-tagged vinblastine) was purchased from Molecular Probes (Invitrogen). The Bradford protein estimation kit was purchased from Genei. All other chemicals were analytical grade.

Purification of Tubulin. Microtubular proteins (MTP) were isolated from goat brain by two cycles of a temperature-dependent polymerization and depolymerization process in PEM buffer [50 mM PIPES (pH 6.9), 1 mM EGTA, and 0.5 mM $MgSO_4$] (*25*). Pure tubulin was isolated from MTP by two additional cycles of a temperature-dependent assembly and disassembly process using 1 M glutamate buffer [1 M glutamate (pH 6.9), 1 mM EGTA, and 0.5 mM $MgSO_4$] for assembly (*25*). Protein aliquots were frozen in liquid nitrogen and stored at −70 °C. The protein concentration was measured by the method of Bradford using bovine serum albumin as the standard (*26*). Unless otherwise stated, all experiments were performed in PEM buffer.

Preparation of the Genistein Solution. The stock solution of genistein was created in DMSO. The concentration of genistein was determined using a molar extinction coefficient of 37300 M^{-1} cm^{-1} at 254 nm in an 80% aqueous methanol solution (*27*). All experiments were conducted via preparation of a secondary solution in PEM buffer in which the final DMSO concentration was < 1%.

Cell Culture. Human lung epithelial carcinoma cells (A549) were maintained in the nutrient mixture F12 Ham supplemented with 1 mM L-glutamine, 10% fetal bovine serum, 50 μg/mL penicillin, 50 μg/mL streptomycin, and 2.5 μg/mL amphotericin B. Cells were cultured at 37 °C in a humidified atmosphere containing 5% CO_2. Cells were grown in tissue culture flasks, until they were 70% confluent before trypsinization with 1× trypsin-versene and splitting. Normal and treated (with 0−100 μM genistein) cell morphology was observed with an Olympus model CKX41 inverted microscope.

Cell Proliferation Inhibition Assay (*MTT Assay*). Inhibition of cell proliferation by genistein was assessed by the MTT [3-(4,5-dimethylthiazolyl-2)-2,5-diphenyltetrazolium bromide] assay. Cells were plated in 96-well culture plates (1×10^4 cells/well). After incubation for 24 h, the cells were treated with genistein (0−100 μM) for 24 h. This was followed by addition of 20 μL of MTT (5 mg/mL) dissolved in PBS, and incubation until a purple precipitate was visible. Subsequently, 100 μL of Triton-X was added, and the mixture was kept in the dark for 4 h at room temperature. The absorbance was measured on an ELISA reader (Multiskan EX, Labsystems, Helsinki, Finland) at a test wavelength of 570 nm and a reference wavelength of 650 nm. Data were calculated as the percentage of inhibition by the following formula:

$$\% \text{ inhibition} = (100 - A_t/A_s \times 100)\% \quad (1)$$

where A_t and A_S represent the absorbance of test sample and solvent control, respectively (*28*).

Cell Cycle Analysis by Flow Cytometry. Cultured A549 cells were seeded at a density of 3×10^4 cells/mL in a 35 mm tissue culture petriplate. The cells were treated with genistein (50, 75, and 100 μM) for 22 h. A set was treated with 0.1 μM paclitaxel for a positive control. After 22 h, the cells were harvested, fixed with ice-cold methanol for 30 min at 4 °C, and incubated for 4 h at 37 °C in a PBS solution containing 1 mg/mL RNase A. Cell cycle analysis was performed using the Becton Dickinson FACScan instrument, and the data were analyzed using Cell Quest from Becton Dickinson.

Mitotic Index. To evaluate mitotic indices, A549 cells were plated at a density of 3×10^4 cells/mL. After 48 h, cells were incubated in the absence or presence of genistein over a range of concentrations (75−100 μM) for 22 h. Media were collected, and cells were rinsed with PBS twice. Cells were fixed with 10% formalin for 30 min, permeabilized in ice-cold methanol for 10 min, and stained with 4,6-diamidino-2-phenylindole (DAPI) (1 μg/mL) to visualize nuclei. Mitotic indices were determined with a Zeiss LSM 510 Meta confocal microscope. Results are means ± SEM of three experiments, in each of which 500 cells were counted at each concentration (*29*).

Immunofluorescence Study. Human lung epithelial carcinoma cells (A549) were seeded on coverslips at a density of 1×10^5 cells/mL and incubated in the presence of different doses of genistein (0−100 μM) for 24 h. Subsequently, genistein-containing medium was removed, and the cells were washed twice with PBS and fixed in 2% paraformaldehyde at room temperature for 1 h. Cell permeable solution (0.1% sodium citrate and 0.1% Triton X-100) was added, and cells were incubated at room temperature for 1 h. Nonspecific binding sites were blocked via incubation of the cells with 5% BSA in PBS overnight at 4 °C. Cells were then incubated with a mouse monoclonal anti-α-tubulin antibody (1:200 dilution) followed by a rhodamine-conjugated anti-mouse secondary antibody (raised in rabbit) (1:150 dilution). After incubation, cells were

[1]Abbreviations: PIPES, 1,4-piperazinediethanesulfonic acid; EGTA, ethylene bis(oxyethylenenitrilo)tetraacetic acid; GTP, guanosine 5′-triphosphate; DTNB, 5,5′-dithiobis(2-nitrobenzoic acid); MTT, 3-(4,5-dimethylthiazolyl-2)-2,5-diphenyltetrazolium bromide; SEM, standard error of the mean; TEM, transmission electron microscope; BODIPY-FL, 4,4-difluoro-3a,4a-diaza-*s*-indacene.

washed twice with PBS, and images were taken using a Zeiss LSM 510 Meta confocal microscope.

Western Blotting. Dimeric tubulin and polymeric tubulin were differentially extracted from cells plated on 35 mm dishes using a modification of the method as described by Minnoti et al. (*30*) for the Western blot experiment. Cultured A549 cells were treated with different concentrations of genistein (0−150 μM) for 24 h. After that, cells were washed twice with PBS, harvested by trypsinization, and lysed at 37 °C for 5 min with 100 μL of extraction buffer [20 mM PIPES (pH 6.8), 0.14 M NaCl, 1 mM $MgCl_2$, 1 mM EGTA, 0.5% NP-40, and 0.5 mM PMSF]. The samples were transferred to microcentrifuge tubes and centrifuged at 16400*g* for 15 min at 4 °C. The supernatant was transferred to a new tube, and polymeric tubulin was extracted from the remaining insoluble material by dissolving the pellet in lysis buffer. The total protein concentrations of the soluble fraction and insoluble fraction were determined by the Bradford method. Equal amounts of protein were loaded in each lane (50 μg for the supernatant and 30 μg in the case of the insoluble fraction) of a 10% SDS−polyacrylamide gel. The samples were then analyzed by Western blotting and probed with an anti-α-tubulin antibody (1:1000 dilution).

Tubulin Polymerization. Tubulin (12 μM) was mixed with different concentrations of genistein (0−100 μM) in polymerization buffer [1 mM $MgSO_4$, 1 mM EGTA, and 1.0 M monosodium glutamate (pH 6.9)], and the polymerization reaction was initiated via addition of 1 mM GTP in the assembly reaction mixture at 37 °C. Tubulin polymerization was monitored by light scattering at 350 nm using a V-630 Jasco spectrophotometer connected to a constant-temperature water circulating bath (*31*).

Transmission Electron Microscope (*TEM*) *Study*. Tubulin (12 μM) was polymerized at 37 °C in the absence and presence of genistein for 30 min. Microtubules were then fixed in 0.5% prewarmed glutaraldehyde for 5 min. Each sample (5 μL) was loaded on carbon-coated grids (300 mesh) for 20 s and blotted dry. The grids were subsequently negatively stained with 1% uranyl acetate and air-dried. The samples in the grids were viewed using a Philips Fei Technai Spirit transmission electron microscope (TEM) (*28*).

Binding Measurements by Fluorescence Spectroscopy. Quenching of the tryptophan fluorescence of tubulin upon genistein binding was used to calculate several binding parameters of tubulin genistein interactions. All fluorescence measurements were performed using a Hitachi fluorescence spectrophotometer (model F-3010) equipped with a constant-temperature water circulating bath. A 1 cm path length quartz cuvette was used for all fluorescence measurements. Fluorescence data were corrected for the inner filter effect according to the equation of Lakowicz (*32*).

$$F_{corr} = F_{obs}\ \text{antilog}[(A_{ex} + A_{em})/2] \quad (2)$$

where A_{ex} is the absorbance at the excitation wavelength and A_{em} is the absorbance at the emission wavelength (*32*). All absorbance measurements were taken using a JASCO V-630 spectrophotometer.

(*i*) *Association Kinetics*. The kinetics of the association reaction of genistein with tubulin was measured under pseudo-first-order conditions (where the ligand was present in a large excess) (*33*, *34*). The tubulin concentration was 1 μM, and the genistein concentration was 20 μM. The ligand was added to the tubulin solution, and emission at 335 nm was measured upon excitation at 295 nm and 37 °C. Excitation and emission slits were 5 and 10 nm, respectively. The quenching data were analyzed according to both monophasic and biphasic equations after correction for the inner filter effect. The best fit was obtained in the case of monophasic analysis:

$$F = Ae^{-k_1 t} + C \quad (3)$$

where F is the fluorescence of the ligand−tubulin complex at time t, A is the amplitude of the monophase, k_1 is the pseudo-first-order rate constant for the reaction, and C is an integration constant. The data were analyzed with Microcal Origin version 7.0. The apparent second-order rate constant was obtained by dividing the observed rate constant for the reaction (k_1) by the ligand concentration.

(*ii*) *Job Plot*. The stoichiometry of protein−ligand binding was determined using the method of continuous variation (*28*, *35*, *36*). Several mixtures of tubulin and genistein were prepared via continuous variation of the concentrations of tubulin and genistein in the mixture, keeping the total concentration of genistein and tubulin constant at 5 μM. Reaction mixtures were incubated at 37 °C for 60 min, and the quenching of tryptophan fluorescence was recorded at 335 nm.

(*iii*) *Dissociation Constant* (K_d). Tubulin (2 μM) was incubated with varying concentrations of genistein (0−25 μM) at 37 °C for 60 min. The fluorescence intensity was measured at 335 nm upon excitation at 295 nm. The apparent decreases in the fluorescence values in the presence of varying concentrations of genistein were corrected for the inner filter effect. The fraction of binding sites (X) occupied by genistein was determined using the equation $X = (F_0 - F)/F_{max}$, where F_0 is the fluorescence intensity of tubulin in the absence of genistein, F is the corrected fluorescence intensity of tubulin in the presence of genistein, and F_{max} is the fluorescence intensity of the fully saturated tubulin−genistein complex, and calculated from the plot of $1/(F_0 - F)$ versus 1/[genistein] and extrapolating 1/[genistein] to zero as shown in Figure 7B. The dissociation constant (K_d) was determined using the relationship (*28*)

$$F_{max}/(F_0 - F) = 1 + K_d/L_f \quad (4)$$

where L_f represents the free genistein concentration ($L_f = C - X$[Y]), C is the total concentration of genistein, and [Y] is the molar concentration of ligand binding sites using a stoichiometry of 1:1 as determined from the Job plot.

Colchicine Binding to Tubulin. To determine whether genistein binds to the colchicine site of tubulin, colchicine binding to tubulin in the presence and absence of genistein was assessed by the fluorescence of the tubulin−colchicine complex (*37*). We prepared samples by mixing 5 μM tubulin with 10 μM colchicine and various concentrations of genistein (5−100 μM). Control samples contained 5 μM tubulin and 10 μM colchicine. The fluorescence of the control sample was compared with those of samples containing both colchicine and genistein.

Vinblastine Binding to Tubulin. To determine whether genistein binds to the vinblastine site of tubulin, the fluorescent analogue of vinblastine, BODIPY-FL-vinblastine, was used. Tubulin (2 μM) was incubated with BODIPY-FL-vinblastine (10 μM) for 20 min at 37 °C. Then genistein was added (0−60 μM) to the preformed tubulin−BODIPY-FL-vinblastine complex and the mixture incubated for 1 h at 37 °C . Fluorescence emission spectra were measured at 500−550 nm upon excitation at 470 nm.

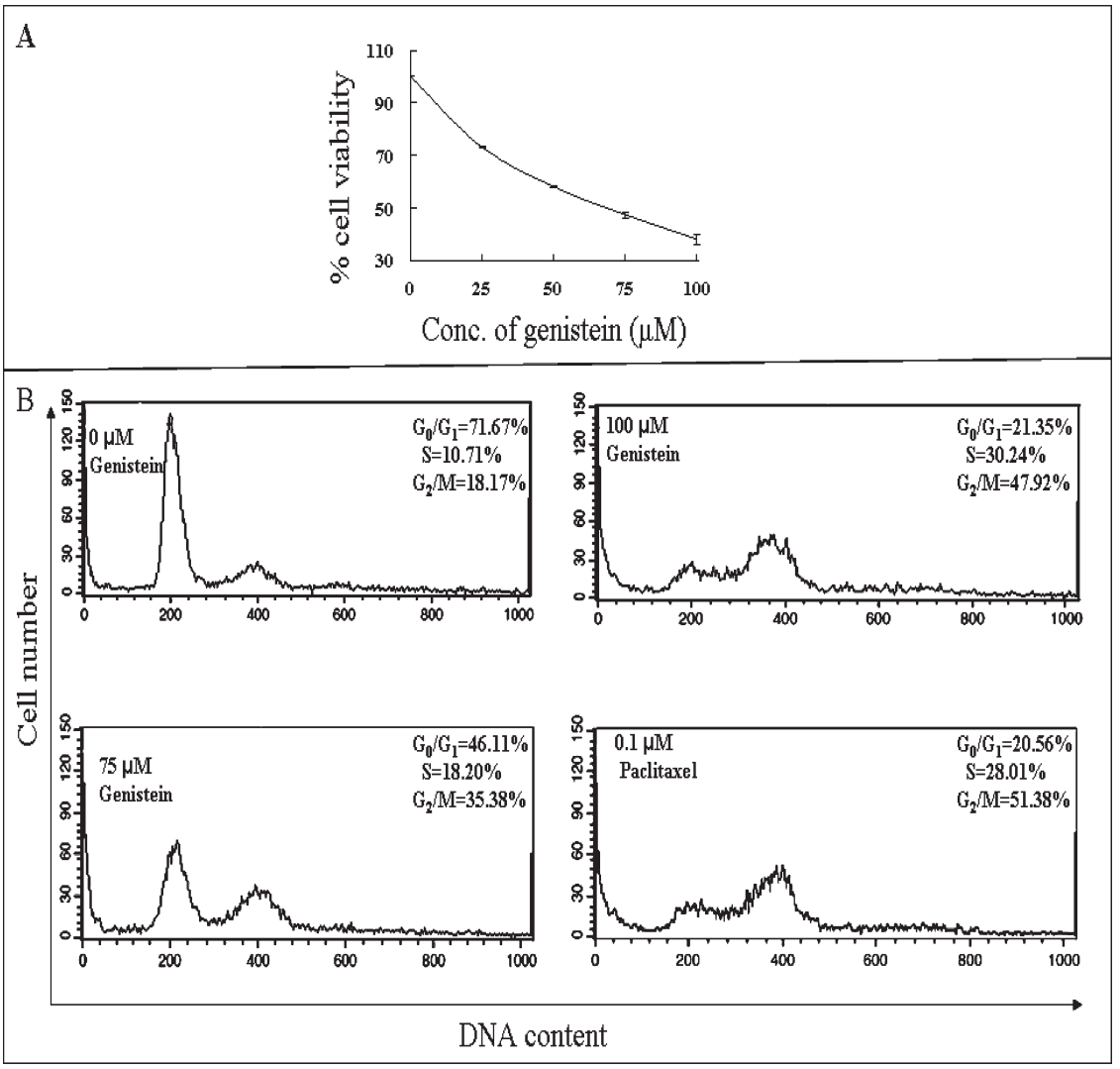

FIGURE 2: (A) Concentration-dependent cell viability assay (MTT assay). Results of the MTT assay with A549 cells treated with 0−100 μM genistein. Details of the experiment are described in Experimental Procedures. (B) Flow cytometric analysis of the cell cycle distribution of A549 cells treated with genistein. Cultured A549 cells were treated with 0, 75, or 100 μM genistein or 0.10 μM paclitaxel separately for 24 h. Cell cycle analysis were conducted using BD FACScaliber, and data were analyzed with Cell Questpro (BD Biosciences).

ANS Binding to Tubulin. The effect of 1-anilino-8-naphthalenesulfonic acid (1,8-ANS) on tubulin−genistein interactions was determined by measurement of the fluorescence of the ANS−tubulin complex. Tubulin was incubated with genistein (0−100 μM) for 60 min at 37 °C to form the tubulin−genistein complex. Then ANS (10 μM) was added to the preformed tubulin−genistein complex and incubated for 30 min at 37 °C. The fluorescence spectra of the samples were recorded at 410−510 nm upon excitation at 370 nm (*38*).

Modified Dixon Plot. A modified Dixon plot for genistein−tubulin binding was obtained using ANS as a competitive inhibitor. ANS binding to tubulin in the presence of genistein was assessed via measurement of the fluorescence of the tubulin−ANS complex. The reaction mixtures containing tubulin (3 μM) and different concentrations of ANS (5−15 μM) and genistein (0−100 μM) were incubated at 37 °C for 45 min. The reciprocal of the fluorescence intensity of the ANS−tubulin complex at 465 nm was plotted against the concentration of genistein. The resulting Dixon plot gave the K_i value for genistein (*28*).

Circular Dichroism Study. Tubulin (3 μM) was incubated with different concentrations (0−100 μM) of genistein in 20 mM sodium phosphate buffer (pH 6.90) for 60 min at 37 °C. Phosphate buffer was used for CD as PIPES had absorbance at 220 nm. The CD spectrum was monitored in the 200−260 nm wavelength region using a cell with a path length of 0.1 cm. All spectra were recorded using a Jasco J 600 spectropolarimeter.

Statistical Analysis. Data are presented as the mean of at least three independent experiments along with the standard error of the mean (SEM). Statistical analysis of the data was done with a Student's *t* test by using MS Excel. Two measurements were statistically significant if the corresponding *p* value was < 0.05.

RESULTS

Genistein Inhibits Proliferation of A549 Cells. Genistein is known to inhibit cell proliferation of human breast cancer cells (MCF-7), human ovarian cancer cells (HeLa), and human prostate cancer cells (PC3) with IC_{50} values of 50 μM (*17*), 100 μM (*37*), and 50 μM (*13*), respectively. We performed the cell viability experiments using human non-small cell lung carcinoma (A549) cells in the presence of genistein by a MTT assay (as explained in Experimental Procedures). Genistein inhibited proliferation of A549 cells in a concentration-dependent manner (Figure 2A). The maximum inhibition of proliferation (62%) was

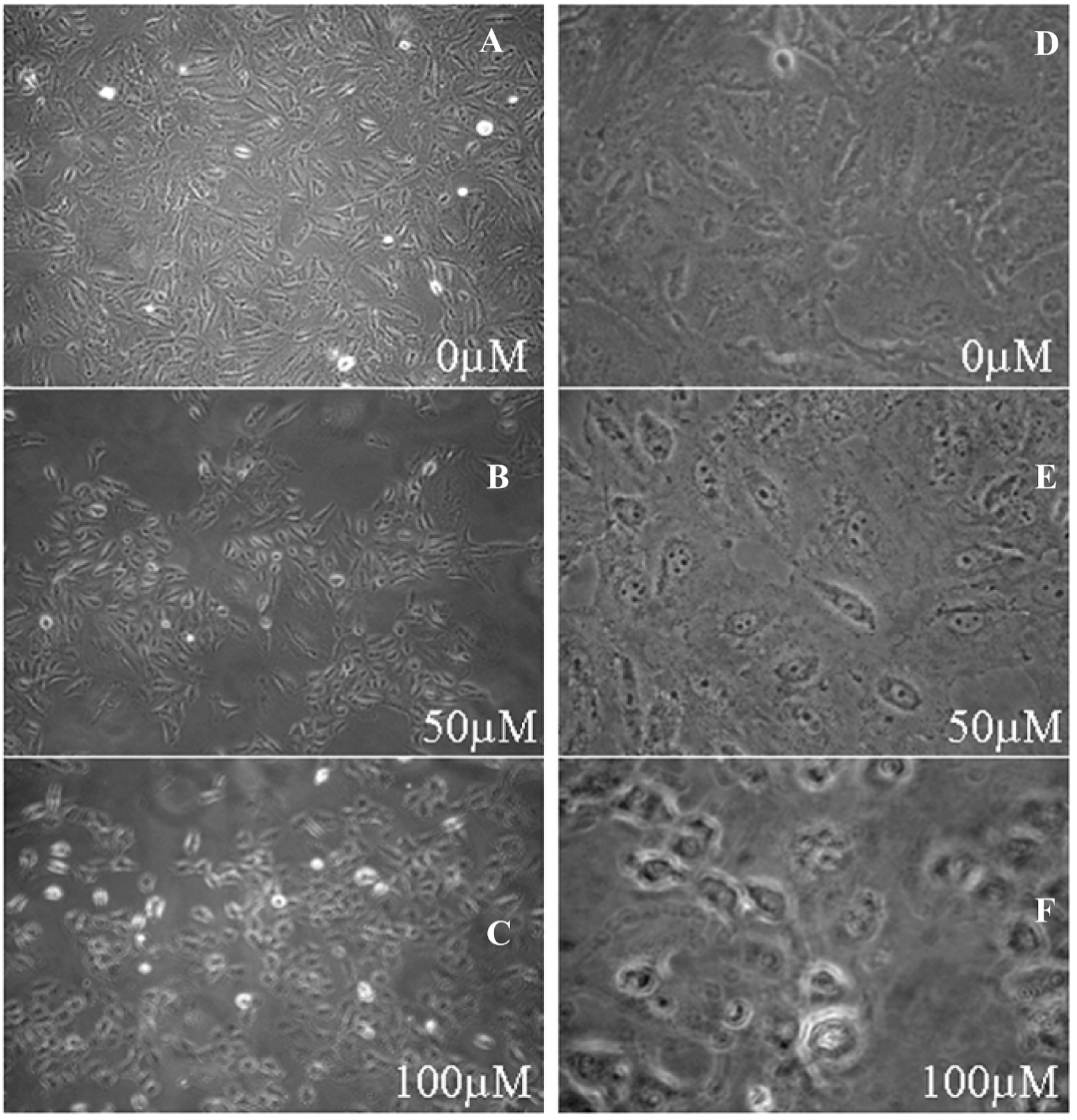

FIGURE 3: Bright field images of genistein-treated A459 cells. Effects of genistein (0−100 μM) on the cellular morphology of A549 cells over 24 h (A−F). Left panels (A−C) are at a lower magnification, and the corresponding right panels (D−F) are at a higher magnification. The pictures were taken with an Olympus inverted microscope (model CKX41).

observed after 24 h with 100 μM genistein, with a calculated IC_{50} value of 72 μM. Thus, our results are comparable with those of other cancer cell lines and support previous observations (*13*, *17*, *37*).

Genistein Induces G_2/M Cell Cycle Arrest of A549 Cells. Genistein is known to arrest human gastric cancer cells (HGC-27) and human breast adeno-carcinoma cells (MCF-7) at the G_2/M phase (*8*, *9*). We have examined the effect of genistein on cell cycle progression of A549 cells by flow cytometric method as shown in Figure 2B. The ratios of untreated cells in G_0/G_1, S, and G_2/M phases of the cell cycle were 71.76, 10.71, and 18.17%, respectively. In the presence of 0.1 μM paclitaxel, the ratios were 20.56, 28.01, and 58.31%, respectively. In the presence of 75 μM genistein, the ratios of the G_0/G_1, S, and G_2/M phases became 46.11, 18.20, and 35.28%, respectively, and in the presence of 100 μM genistein, the ratios were 21.35, 30.24, and 47.92%, respectively. These results indicate that the percentage of cells in the G_2/M phase increased in a dose-dependent manner compared to that of untreated cells and comparable with that of paclitaxel-treated cells. Thus, genistein arrests the A549 cell cycle at the G_2/M phase.

Mitotic Index. To determine whether genistein arrested the cell cycle progression at mitosis, we have calculated mitotic indices of untreated and genistein-treated cells using confocal microscopy (details in Experimental Procedures). The ratios of mitotic cells in the presence of 75 and 100 μM genistein (after incubation for 24 h) were 3.04 ± 0.64 and 2.77 ± 1.34% [standard deviation (SD); $n = 3$, total of 500 cells], respectively, compared to 3.87 ± 0.32% (SD; $n = 3$, total of 500 cells) for untreated control cells. These results, including flow cytometric analysis, suggest that genistein arrested the cell cycle at the G_2 phase rather than at the M phase because there was no increase in the mitotic index. This observation is corroborated by the observation of Matsukawa et al. (*8*), who found that genistein arrests cell cycle progression of human gastric cancer cells (HGC-27) at the G_2 phase.

Genistein Alters the Cellular Morphology of A549 Cells. Genistein has been shown to arrest the cell cycle at the G_2/M phase and induce apoptosis of cancer cell lines (*8*, *9*). The effect of genistein on the cellular morphology of lung epithelium carcinoma (A549) cells was examined by inverted microscopy (Olympus, model CKX41). Lung epithelium carcinoma (A549) cells were incubated in the presence of different concentrations of genistein (0−100 μM) for 24 h, and then bright field images of the treated cells were taken (Figure 3). Aberrations in cellular morphology

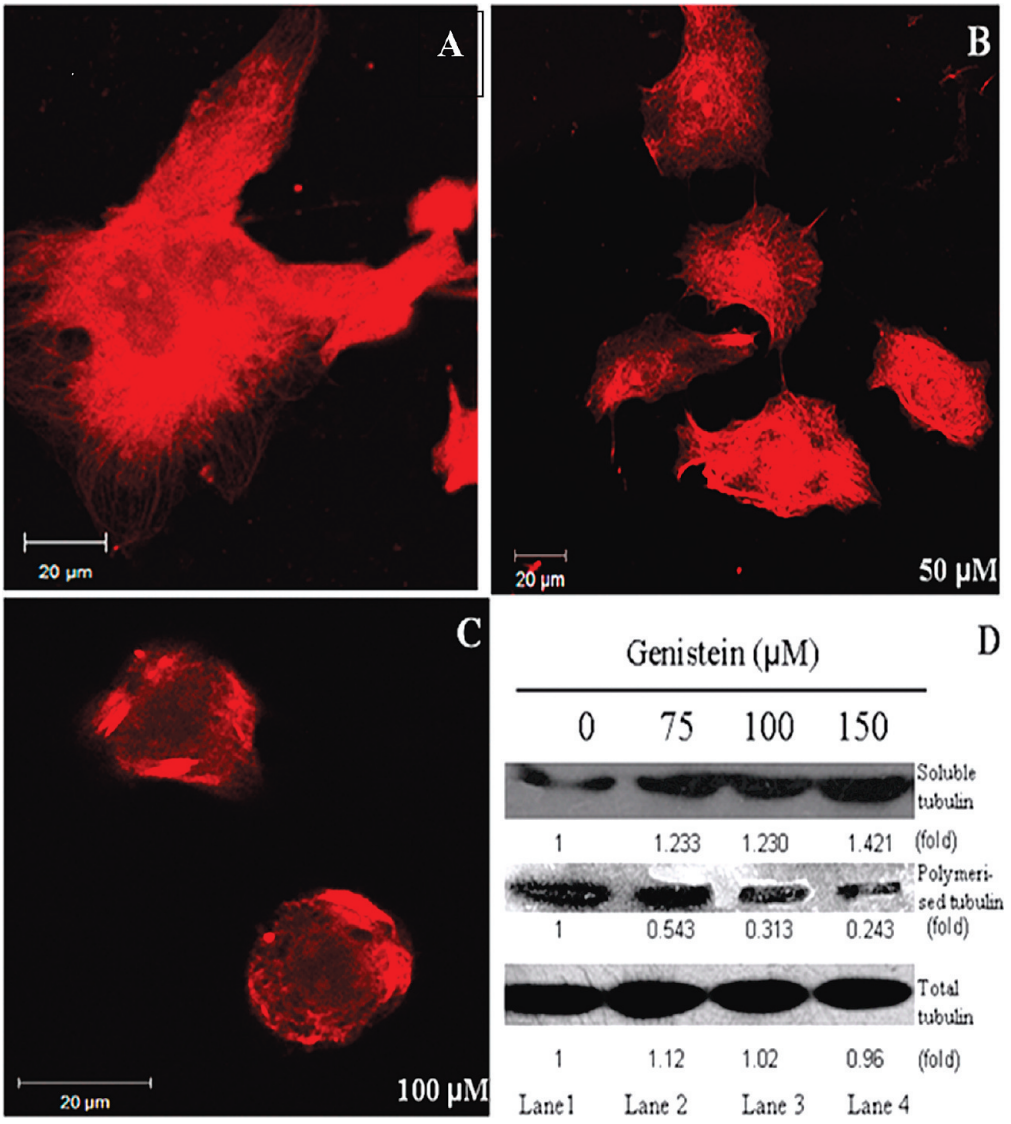

FIGURE 4: Immunofluorescence study of interphase microtubule disruption of A549 cells by genistein. Effects of (0−100 μM) genistein on microtubule networks of A549 cells in different fields (A−C). Controls were solvent (0.1% DMSO)-treated cells (A). Microtubules are tagged with the monoclonal anti-α-tubulin antibody (mouse) and rhodamine (red)-conjugated anti-mouse secondary antibody. Details of the experiment are given in Experimental Procedures. (D) Effect of genistein on tubulin polymerization in A549 cells. Cultured A459 cells were treated with 0, 75, 100, and 150 μM genistein over an 24 h period. Cells were lysed with a hypotonic lysis buffer. Following cell lysis, the polymerized and soluble forms of tubulin were separated by centrifugation. Western blot analysis was conducted using a mouse monoclonal antibody against α-tubulin. The band intensities were measured with a densitometer.

were observed. At 25 μM genistein, there were no significant changes in the morphology of the cells. Cell shapes started changing above 50 μM, and cells became largely round in shape at 100 μM genistein (Figure 3). These results established that genistein is responsible for the alteration in the cellular morphology of A549 cells.

Depolymerization of the Microtubule Network of A549 Cells by Genistein. Since the tubulin−microtubule equilibrium plays a critical role in maintaining the cellular morphology and genistein significantly altered the morphology of A549 cells (Figure 3), we, therefore, were interested in examining whether genistein targeted the microtubule network in lung epithelium carcinoma (A549) cultured cells. This was monitored by confocal microscopy using an anti-α-tubulin antibody (Figure 4) (described in Experimental Procedure). Control cells exhibited regular organized microtubules. No effect of genistein on the microtubule network was apparent at a low concentration (25 μM) of genistein (data not shown). However, at higher concentrations of genistein (50 μM), a significant reduction in the number of microtubules at the periphery of the cells occurred. Genistein greatly disrupted interphase microtubules in A549 cells at a concentration of 100 μM.

We also checked the effect of genistein on spindle microtubules in A549 cells by confocal microscopy using an anti-α-tubulin antibody. Because genistein arrests the cell cycle at the G_2 phase and not at mitosis, we observed very few spindle microtubules in the presence of different concentrations of genistein. Genistein had no significant effect on spindle microtubules of A549 cells (data not shown).

Genistein Reduces the Polymerized Microtubule Mass in A549 Cells. To quantify the effect of genistein on microtubule mass in A549 cells, Western blot analysis using an anti-α-tubulin antibody were performed for both soluble tubulin and assembled tubulin of A549 cells after treatment with genistein. As shown in Figure 4D, the amount of soluble tubulin in genistein-treated cells increased in a concentration-dependent manner compared

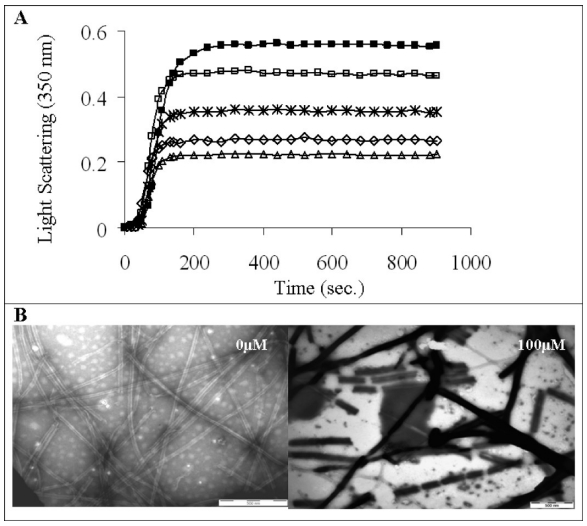

FIGURE 5: Effect of genistein on tubulin assembly. (A) Tubulin (12 μM) was mixed with genistein at different concentrations: 0 (■), 50 (□), 75 (×), 90 (◇), and 100 μM (△) in GEM buffer at 37 °C. Tubulin assembly was monitored by measuring the light scattering at 350 nm. (B) Microtubules in the absence (left) and presence (right) of 100 μM genistein as visualized with an electron microscope. Images were taken at 63000× magnification for the control and 26000× magnification for the sample treated with 100 μM genistein. Details of the assembly reaction and electron microscopy are described in Experimental Procedures.

to that of control cells (untreated cells). Cells treated with 75, 100, and 150 μM genistein also exhibited a decreased amount of the polymer mass of tubulin (Figure 4D, lanes 2−4), while total tubulin remained unchanged. These results indicate that genistein depolymerizes microtubules in A549 cells.

Inhibition of Tubulin Polymerization into Microtubules by Genistein in Vitro. Since genistein affects the cellular morphology of the cells by disrupting the interphase microtubule network, the effect of genistein on tubulin polymerization was tested using purified tubulin via a light scattering assay (as explained in Experimental Procedures). Purified tubulin (12 μM) was polymerized in the absence or presence of different concentrations of genistein, and the results of such experiments are shown in Figure 5A. Genistein inhibited the tubulin polymerization in a concentration-dependent manner. For example, the level of inhibition of tubulin polymerization was 60% at 100 μM genistein and 50% (IC_{50}) at 87 ± 0.5 μM genistein.

The inhibition of tubulin polymerization in the presence of genistein, as monitored by light scattering assay, could be due to the formation of very short microtubules, an altered polymer morphology, or the formation of small aggregates of tubulin. To differentiate among these possibilities, reaction products formed in the presence of genistein were examined with a transmission electron microscope. In the absence of genistein (control experiment), tubulin polymerized in 1 M glutamate buffer formed normal long microtubules, which is consistent with previous reports (*25*) (Figure 5B). After genistein (100 μM) treatment, long microtubules were replaced with short ones. These results indicate that genistein inhibits tubulin polymerization in vitro.

The IC_{50} value of genistein for in vitro tubulin (12 μM) polymerization inhibition is 87 μM. Under similar conditions, the IC_{50} value for colchicine is 3 μM (data not shown), indicating the substoichiometric inhibition of tubulin polymerization by colchicine. For genistein, the IC_{50} value is 87 μM, which is 7−8-fold higher than the tubulin concentration present in the reaction mixture. We therefore concluded that the inhibition of tubulin polymerization by colchicine and genistein does not follow the same mechanism and needs further study.

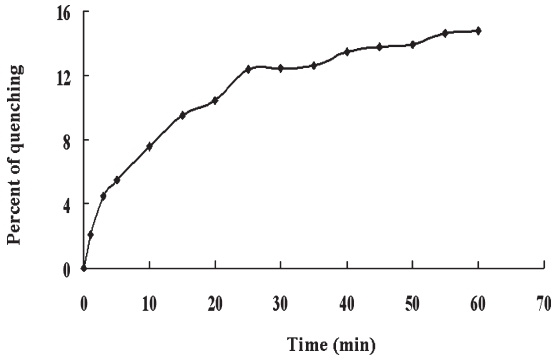

FIGURE 6: Kinetics of genistein binding to tubulin. Percent of quenching of tryptophan fluorescence of tubulin upon binding of genistein to tubulin. Tubulin (1 μM) in PEM buffer was mixed with 20 μM genistein. Kinetics was followed for ∼1 h at 37 °C by measuring the intensity of the intrinsic protein fluorescence at 335 nm upon excitation at 295 nm. Data are represented as means ± SEM ($P < 0.05$; $n = 3$).

Binding of Genistein to Tubulin. Although both genistein and ANS (Figure 1) contain aromatic ring and bear structural similarity, unlike ANS, genistein shows no fluorescence in the presence of proteins. However, the absorption spectra of genistein are extended and overlap with the fluorescence emission spectra of tryptophans of tubulin (Figure 1). Tubulin contains 12 tryptophan residues, which are distributed in α- and β-subunits of tubulin. The binding of genistein to tubulin quenches its tryptophan fluorescence. Therefore, the binding of genistein to tubulin has been studied by measuring the quenching of the intrinsic tryptophan fluorescence of tubulin. Genistein quenches tryptophan fluorescence in a time- and concentration-dependent manner. Addition of 20 μM genistein to tubulin (1 μM) quenches ∼15−18% of its tryptophan fluorescence during 45 min incubation at 37 °C. Therefore, the association rate constant of genistein binding to tubulin was determined by ligand-induced quenching of tubulin fluorescence. Figure 6 shows the time-dependent binding of genistein to tubulin under pseudo-first-order conditions at 37 °C . The quenching data were analyzed using a single-exponential equation as explained in Experimental Procedures. The apparent second-order rate constant has been found to be 104.64 ± 20.63 M^{-1} s^{-1} at 37 °C. Time-dependent quenching indicates the specificity of binding which is very similar to that of the colchicine−tubulin interaction. However, unlike that of colchicine, there is no blue shift in the emission maximum of tubulin upon binding with genistein.

The stoichiometry and the dissociation constant (K_d) of the tubulin−genistein interaction have been determined by measuring the tryptophan quenching of tubulin upon genistein binding. The stoichiometry of genistein−tubulin binding was calculated from the Job plot. In this plot, concentrations of both tubulin and genistein were varied while the total ligand and protein concentration was kept fixed at 5 μM. Results of such experiments are presented in Figure 7A. The stoichiometry of binding has been found to be 1:1 using the Job plot of continuous variation (*35*, *36*).

The determination of the dissociation constant (K_d) has been described in detail in Experimental Procedures. Figure 7B shows the quenching profile of a fixed concentration of tubulin (1 μM) with various concentrations of genistein (0−25 μM) at 37 °C. The dissociation constant has been determined from eq 4 and from

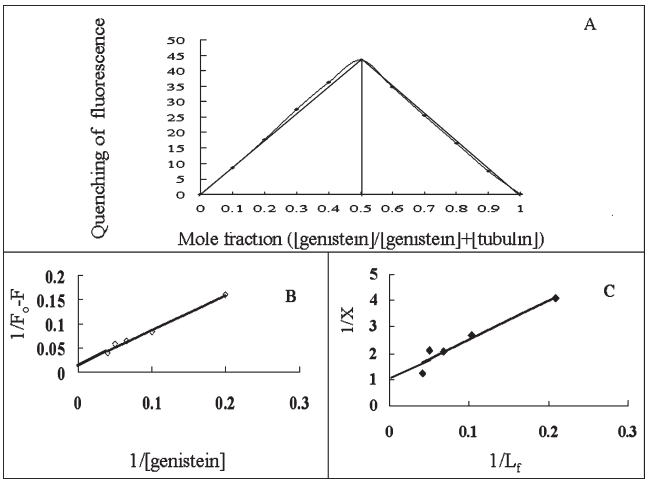

FIGURE 7: Characterization of genistein binding to tubulin. (A) Job plot of genistein binding to tubulin. The concentrations of tubulin and genistein were varied continuously while the total concentration of genistein and tubulin was kept constant at 5 μM. The quenching of fluorescence intensities at 335 nm corrected for the inner filter effect is plotted against the mole fraction of genistein. Data are represented as means ± SEM ($P < 0.05$; $n = 3$). (B) Double-reciprocal plot of genistein binding to tubulin. F_{max} is calculated from the graph of $1/(F_0 - F)$ vs 1/[genistein]. (C) Double-reciprocal plot of genistein binding to tubulin. Data are represented as means ± SEM ($P < 0.05$; $n = 4$). Data are representative of four identical experiments.

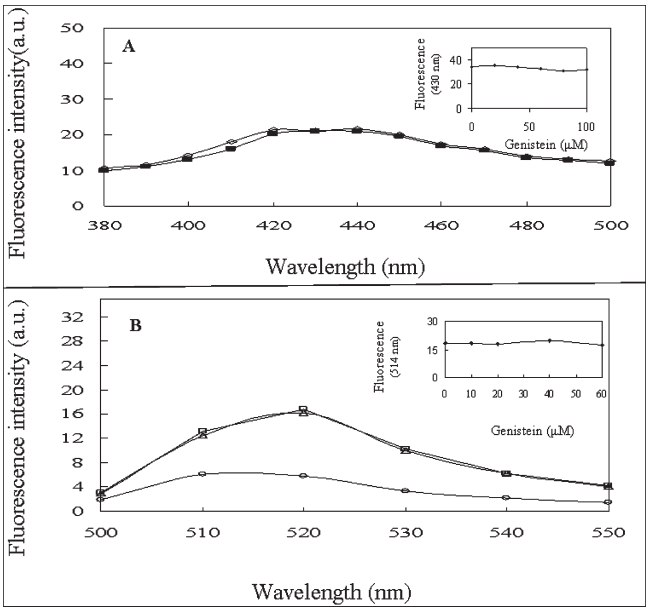

FIGURE 8: Effect of genistein on colchicine binding and vinblastine binding to tubulin. (A) Tubulin (5 μM) was incubated with colchicine (10 μM) in the absence (□) and presence (◇) of 100 μM genistein at 37 °C for 1 h. Fluorescence emission spectra were recorded upon excitation at 340 nm. The inset shows the fluorescence intensity at 430 nm vs genistein concentration. (B) Tubulin (2 μM) was incubated with BODIPY-FL-vinblastine (10 μM) for 20 min at 25 °C; 60 μM genistein was added, and the mixture was incubated at 37 °C for 1 h. Fluorescence emission spectra were recorded upon excitation at 470 nm. The fluorescence of BODIPY-FL-vinblastine (◇), the BODIPY-FL-vinblastine−tubulin complex (□), and the BODIPY-FL-vinblastine−tubulin−genistein complex (△) is plotted. The inset shows the fluorescence at 514 nm vs genistein concentration.

the reciprocal plot as shown in Figure 7C. The analysis of data yielded a dissociation constant (K_d) of 15 ± 1.3 μM.

Genistein Does Not Compete for the Colchicine Binding Site of Tubulin. Quenching of the tryptophan fluorescence of tubulin upon genistein binding is slow at 37 °C and resembles that of the colchicine−tubulin interaction. We, therefore, tested whether genistein competes for the colchicine site of tubulin. Colchicine does not fluoresce in aqueous solution, but it fluoresces when bound to tubulin (*37*). We used the colchicine−tubulin complex fluorescence to determine whether genistein binds at the colchicine site of tubulin. For this purpose, samples contained tubulin (5 μM), a fixed concentration of colchicine (10 μM), and varied concentrations of genistein (0−100 μM). All samples were incubated at 37 °C for 1 h. The fluorescence of complexes was measured from 380 to 500 nm upon excitation at 350 nm (Figure 8A). Genistein has no effect on the colchicine−tubulin interaction. These results indicate that the genistein binding site is different from that of the colchicine binding site of tubulin.

Genistein Does Not Bind to the Vinblastine Binding Site in Tubulin. There are three distinct, well-defined antimitotic drug binding sites on tubulin. These are paclitaxel, colchicine, and vinblastine sites. Drugs binding to the paclitaxel site stimulate tubulin polymerization, while drugs binding to either the colchicine or vinblastine site inhibit polymerization. Like colchicine and vinblastine, genistein inhibits tubulin polymerization. However, genistein does not compete for the colchicine site of tubulin. We, therefore, checked whether genistein binds to the vinblastine site of tubulin. For this purpose, a fluorescent analogue of vinblastine called BODIPY-FL-vinblastine has been used, which inhibits tubulin polymerization in a manner similar to that of vinblastine (data not shown). Binding to tubulin enhanced its fluorescence significantly. Figure 8B shows the fluorescence emission spectra of BODIPY-FL-vinblastine in the absence and presence of tubulin. We prepared several identical samples containing a fixed concentration of tubulin (2 μM) and BODIPY-FL-vinblastine (10 μM) by incubating them for 20 min at 37 °C. We recorded their fluorescence, and then various concentrations (0−60 μM) of genistein were added to these preformed complexes and the mixtures again incubated for 60 min at 37 °C. The fluorescence was measured from 500 to 550 nm upon excitation at 475 nm (Figure 8B). From the results, it is clear that genistein does not bind to the vinblastine site of tubulin.

Genistein Competes for the ANS Binding Site of Tubulin. Several aminonaphthalenes, including 1,8-anilinonaphthalenesulfonate (1,8-ANS), bind tubulin and inhibit microtubule formation in vitro (*38*, *39*). It was suggested that tubulin contains a single high-affinity binding site of ANS that is responsible for the inhibition of tubulin polymerization. Since both ANS and genistein bear structural similarity, we are curious to know whether genistein affects the binding of ANS to tubulin. ANS has very weak fluorescence in aqueous solution, but its fluorescence increases severalfold upon binding to tubulin (*38*). To see the effect of genistein on ANS−tubulin fluorescence, ANS (10 μM) was added to the preformed tubulin−genistein complex containing 2 μM tubulin and various concentrations of genistein. The emission spectra were recorded between 410 and 510 nm upon excitation at 370 nm. Results of such experiments are shown in Figure 9A. Genistein quenches the fluorescence of the tubulin−ANS complex in a concentration-dependent manner, and 90 μM genistein quenches tubulin−ANS fluorescence nearly 40%. To determine whether genistein binds at the ANS site of tubulin, ANS was allowed to compete with genistein for binding to tubulin, and the data were analyzed using a modified Dixon

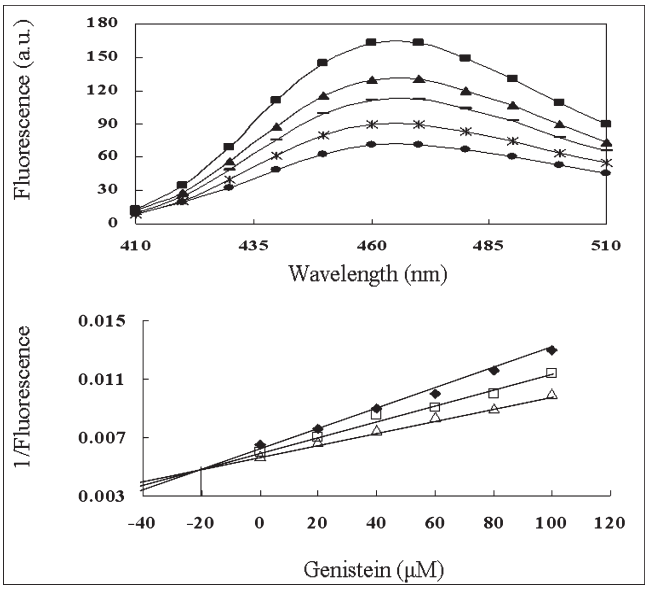

FIGURE 9: Genistein inhibited the binding of ANS to tubulin. (A) Quenching of the tubulin−ANS complex fluorescence by genistein. Tubulin (2 μM) was mixed with ANS (10 μM) and concentrations of genistein [0 (■), 20 (▲), 40 (—), 80 (×), and 100 μM (●)] and incubated for 1 h. The excitation wavelength was 370 nm, and the emission fluorescence spectra were recorded from 410 to 510 nm. Data are representative of three replicate experiments. (B) Modified Dixon plot. The concentrations of ANS were 10 (◆), 15 (□), and 20 μM (△). The reaction mixture contained tubulin (2 μM) and genistein at the indicated concentration (0−100 μM), and they were incubated at 37 °C for 1 h. Data are represented as means ± SEM ($P < 0.05$; $n = 3$).

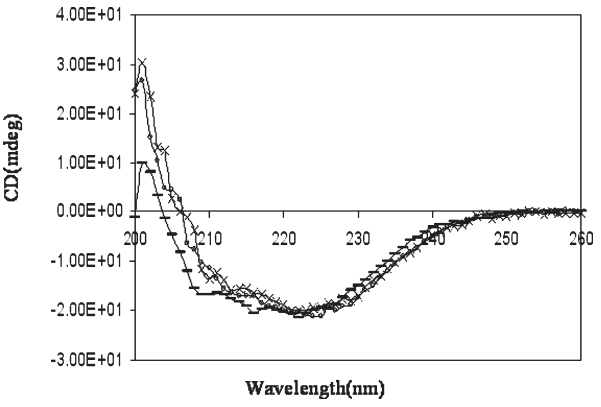

FIGURE 10: Far-UV CD spectra of 3 μM tubulin in the absence (−) and presence of 50 (◇) and 100 μM (×) genistein in 20 mM phosphate buffer (pH 6.8).

plot (Figure 9B). The binding was studied fluorometrically using ANS fluorescence. The results presented in Figure 9B clearly indicate that genistein inhibits competitively binding of ANS to tubulin with a K_i value of 20 μM.

Effect of Genistein on the CD Spectrum of Tubulin. The effect of genistein on the secondary structure of tubulin has been monitored by CD spectroscopy, and the data are presented in Figure 10. Genistein has no effect on the secondary structure of tubulin.

DISCUSSION

Genistein, an isoflavanoid, has been shown to inhibit proliferation of several cancer cell types . However, the mechanism of its action is not clearly understood (*12*−*15*). In this study, we have examined the effect of genistein on human non-small lung carcinoma (A549) cells. Here we observed that genistein inhibits cell proliferation and arrests cell cycle progression at the G_2 phase but not at mitosis. Genistein treatment also altered the morphology of A549 cells along with depolymerization of microtubules. In vitro, genistein inhibited polymerization of purified tubulin into microtubules. A cell viability experiment using human non-small lung epithelium cell carcinoma (A549) cells indicated that the IC_{50} value for genistein is 72 μM, and this value was consistent with the reported values using other cell lines (*13*, *17*, *40*). Flow cytometry studies indicated that genistein arrests cell cycle progression at the G_2/M phase, and treatment of A549 cells with genistein caused a decrease in the level of expression of cyclin B1 and cdc25B (data not shown), which also indicates G_2/M phase arrest. However, mitotic index data indicated that genistein did not arrest cell cycle progression at mitosis, and this is corroborated by the observation of Matsukawa et al. (*8*). Immunofluorescence and Western blot studies using an anti-α-tubulin antibody indicated that depolymerization of the interphase microtubule network of A549 cells in the presence of genistein occurred in a concentration-dependent manner. Most of the agents, which target microtubules in cells, arrest cell cycle progression at mitosis, but there is evidence that at higher concentrations, colchicine, nocadazole, and vincristine depolymerize microtubules in cells and arrest cell cycle progression at the G_2 phase (*41*). The reason for G_2 phase arrest is not clear but could be related to the upregulation of p21 (*41*). Blajeski et al. observed that treatment of some cells with colchicine, nocadazole, and vincristine at higher concentrations upregulates p21 expression, which initiates cell cycle arrest at the G_2 phase and escapes the cell cycle progression at mitosis (*41*). Upregulation of p21 in A549 cells in the presence of genistein was reported (*42*).

From this discussion, it is clear that genistein inhibits cancer cell proliferation, alters their morphology, and depolymerizes interphase microtubules. The obvious question, therefore, is where genistein binds to tubulin. Is it one of the well-established sites such as the colchicine or vinblastine site of tubulin? Like colchicine, genistein binds to tubulin slowly at 37 °C and equilibrates in ~45 min. Surprisingly, competition experiments clearly established that genistein did not compete for the colchicine binding site of tubulin. Although genistein does not fluoresce upon binding to tubulin, it does quench the tryptophan fluorescence of tubulin. The association rate constant as determined using tryptophan fluorescence quenching has been found to be 104.64 ± 20.63 M^{-1} s^{-1} at 37 °C . The dissociation constant (K_d) was determined for the genistein−tubulin interaction and found to be 14.94 ± 1.3 μM at 37 °C. Vinblastine is another antimitotic drug that binds tubulin and inhibits tubulin self-assembly. We, therefore, tested whether genistein binds to the vinblastine site of tubulin. We used fluorescence-labeled vinblastine (BODIPY-FL-vinblastine) for our study. Preincubation of tubulin with a high concentration of genistein does not affect the fluorescence of the vinblastine−tubulin complex. Addition of a high concentration of genistein to the preformed tubulin−vinblastine complex also has no effect. We, therefore, concluded that genistein recognizes neither the colchicine binding site nor the vinblastine binding site of tubulin. Drugs bound to the paclitaxel site of tubulin generally promote self-assembly and stabilize microtubules. We, therefore, have not tested the effect of genistein on the binding of paclitaxel to tubulin.

Aminonaphthalene drugs and their analogues like ANS and bis-ANS also bind to tubulin and inhibit its polymerization into

microtubules (*36*, *41*). Both genistein and ANS are structurally similar, containing an aromatic ring system (Figure 1). Therefore, it is possible that genistein recognizes the aminonaphthalene binding site of tubulin. A modified Dixon plot showed that genistein inhibits ANS binding and competes for the ANS binding site of tubulin with a K_i of 20 μM. This aminonaphthalene site of tubulin is not well established like colchicine, vinblastine, or paclitaxel site of tubulin. However, in past few years, a large number of antimitotic agents were discovered, but their binding site on tubulin or another receptor is yet to be explored.

Finally, genistein, which is currently in a phase II clinical trial (*15*), is an important addition to the list of potential antimitotic drugs because of its low toxicity. Further development using genistein as a lead compound needs to screen a large number of its analogues and finally the crystal structure of the tubulin−genistein complex.

ACKNOWLEDGMENT

We thank Prof. I. B. Chattaerjee of this department for critical reading and suggestions for preparation of the manuscript. We also thank Mr. Sailen Dey (Indian Institute of Chemical Biology, Kolkata, India) for technical assistance during the TEM study. The confocal microscope facility was developed with a grant from the National Common Minimum Program, Government of India.

REFERENCES

1. Wiltrout, R. H., and Hornung, R. L. (1988) Natural products as antitumor agents: Direct versus indirect mechanisms of activity of flavonoids. *J. Natl. Cancer Inst. 80*, 220–222.
2. Agullo, G., Gamet-Payrastre, L., Fernandez, Y., Anciaux, N., Demigne, C., and Remesy, C. (1996) Comparative effects of flavonoids on the growth, viability and metabolism of a colonic adenocarcinoma cell line (HT29 cells). *Cancer Lett. 105*, 61–70.
3. Beutler, J. A., Hamel, E., Vlietinck, A. J., Haemers, A., Rajan, P., Roitman, J. N., Cardellina, J. H., II, and Boyd, M. R. (1998) Structure-activity requirements for flavone cytotoxicity and binding to tubulin. *J. Med. Chem. 41*, 2333–2338.
4. Lamson, D. W., and Brignall, M. S. (1999) Antioxidants in cancer therapy: Their actions and interactions with oncologic therapies. *Altern. Med. Rev. 4*, 304–329.
5. Kobayashi, T., Nakata, T., and Kuzumaki, T. (2002) Effect of flavonoids on cell cycle progression in prostate cancer cells. *Cancer Lett. 176*, 17–23.
6. Ikegawa, T., Ohtani, H., Koyabu, N., Juichi, M., Iwase, Y., Ito, C., Furukawa, H., Naito, M., Tsuruo, T., and Sawada, Y. (2002) Inhibition of P-glycoprotein by flavonoid derivatives in adriamycin-resistant human myelogenous leukemia (K562/ADM) cells. *Cancer Lett. 177*, 89–93.
7. Shon, Y. H., Park, S. D., and Nam, K. S. (2006) Effective Chemopreventive Activity of Genistein against Human Breast Cancer Cell. *J. Biochem. Mol. Biol. 39*, 448–451.
8. Matsukawa, Y., Marui, N., Sakai, T., Satomi, Y., Yoshida, M., Matsumoto, K., Nishino, H., and Aoike, A. (1993) Genistein Arrests Cell Cycle Progression at G2-M. *Cancer Res. 53*, 1328–1331.
9. Constantinou, A. I., Kamath, N., and Murley, J. S. (1998) Genistein inactivates bcl-2, delays the G2/M phase of the cell cycle, and induces apoptosis of human breast adeno-carcinoma MCF-7 cells. *Eur. J. Cancer 34*, 1927–1934.
10. Lamartiniere, C. A., Cotroneo, M. S., Fritz, W. A., Wang, J., Mentor-Marcel, R., and Elgavish, A. (2002) Genistein Chemoprevention: Timing and Mechanisms of Action in Murine Mammary and Prostate. *J. Nutr. 132*, 552S–558S.
11. Barnes, S. (1997) The chemopreventive properties of soy isoflavonoids in animal models of breast cancer. *Breast Cancer Res. Treat. 46*, 169–179.
12. Fritz, W. A., Coward, L., Wang, J., and Lamartiniere, C. A. (1998) Dietary genistein: Perinatal mammary cancer prevention, bioavailability and toxicity testing in the rat. *Carcinogenesis 19*, 2151–2158.
13. Onozawa, M., Fukuda, K., Ohtani, M., Akaza, H., Sugimura, T., and Wakabayashi, K. (1998) Effects of soybean isoflavones on cell growth and apoptosis of the human prostatic cancer cell line LNCaP. *Jpn. J. Clin. Oncol. 28*, 360–363.
14. Zhou, J. R., Mukherjee, P., Gugger, E. T., Tanaka, T., Blackburn, G. L., and Clinton, S. K. (1998) Inhibition of murine bladder tumorigenesis by soy isoflavones via alterations in the cell cycle, apoptosis, and angiogenesis. *Cancer Res. 58*, 5231–5238.
15. Pendleton, J. M., Tan, W. W., Anai, S., Change, M., Hou, H., Shiverick, K. T., and Rosser, C. J. (2008) Phase II trial of isoflavone in prostate-specific antigen recurrent prostate cancer after previous local therapy. *BMC Cancer 8* (132), 1–10.
16. Lian, F., Li, Y., Bhuiyan, M., and Sarkar, F. H. (1999) p53-independent apoptosis induced by genistein in lung cancer cells. *Nutr. Cancer 33*, 125–131.
17. Li, Y., Upadhyay, S., Bhuiyan, M., and Sarkar, F. H. (1999) Induction of apoptosis in breast cancer cells MDA-MB-231 by genistein. *Oncogene 18*, 3166–3172.
18. Shao, Z. M., Alpaugh, M. L., Fontana, J. A., and Barsky, S. H. (1998) Genistein inhibits proliferation similarly in estrogen receptor positive and negative human breast carcinoma cell lines characterized by p21WAF1/CIP1 induction, G2/M arrest, and apoptosis. *J. Cell. Biochem. 69*, 44–54.
19. Akiyama, T., Ishida, J., Nakagawa, S., Ogawara, H., Watanabe, S., Itoh, N., Shibuya, M., and Fukami, Y. (1987) Genistein, a specific inhibitor of tyrosine-specific protein kinases. *J. Biol. Chem. 262*, 5592–5595.
20. Markovits, J., Linassier, C., Fossé, P., Couprie, J., Pierre, J., Jacquemin-Sablon, A., Saucier, J. M., Le Pecq, J. B., and Larsen, A. K. (1989) Inhibitory Effects of the Tyrosine Kinase Inhibitor Genistein on Mammalian DNA Topoisomerase II. *Cancer Res. 49*, 5111–5117.
21. Davis, J. N., Singh, B., Bhuiyan, M., and Sarkar, F. H. (1998) Genistein-induced upregulation of p21WAF1, downregulation of cyclin B, and induction of apoptosis in prostate cancer cells. *Nutr. Cancer 32*, 123–131.
22. Gupta, K., and Panda, D. (2002) Perturbation of microtubule polymerization by quercetin through tubulin binding: A novel mechanism of its antiproliferative activity. *Biochemistry 41*, 13029–13038.
23. Lodish, H., Baltimore, D., Berk, A., Zipursky, S. L., Matsudaira, P., and Darnell, J. (1999) Molecular and Cellular Biology, W. H. Freeman, New York.
24. Jordan, M. A., and Wilson, L. (2004) Microtubules as a target for anticancer drugs. *Nat. Rev. Cancer 4*, 253–265.
25. Hamel, E., and Lin, C. M. (1981) Glutamate-induced polymerization of tubulin: Characteristics of the reaction and application to the large-scale purification of tubulin. *Arch. Biochem. Biophys. 209*, 29–40.
26. Bradford, M. M. (1976) A rapid and sensitive method for the quantitation of microgram quantities of protein utilizing the principle of protein-dye binding. *Anal. Biochem. 72*, 248–254.
27. Maheshal, H. G., Singh, S. A., Srinivasan, N., and Rao, A. (2006) A spectroscopic study of the interaction of isoflavones with human serum albumin. *FEBS J. 273*, 451–467.
28. Acharya, B., Bhattacharyya, B., and Chakrabarti, G. (2008) The natural naphthoquinone plumbagin exhibits antiproleferative acivity and disrupts the microtubule network through tubulin binding. *Biochemistry 47*, 7838–7845.
29. Kamath, K., and Jordon, M. A. (2003) Suppression of microtubule dynamics by Epothilone B is associated with mitotic arrest. *Cancer Res. 63*, 6026–6031.
30. Minnoti, A. M., Barlow, S. B., and Cabral, F. (1991) Resistance to antimitotic drugs in Chinese hamster ovary cells correlates with changes in the level of polymerized tubulin. *J. Cell. Biochem. 266*, 3987–3994.
31. Gaskin, F., Cantor, C. R., and Shelanski, M. L. (1974) Turbidimetric studies of the in vitro assembly and disassembly of porcine neurotubules. *J. Mol. Biol. 89*, 737–755.
32. Lakowicz, J. R. (1999) Principles of Fluorescence Spectroscopy, 2nd ed., Kluwer Academic/Plenum Publishers, New York.
33. Chakrabarti, G., Sengupta, G., and Bhattacharyya, G. (1996) Thermodynamics of Colchicinoid-Tubulin Interactions: Role of B ring and C7 substituent. *J. Biol. Chem. 271*, 2897–2901.
34. Pyles, A. E., and Bane, S. H. (1993) Effect of the B ring and the C-7 substituent on the kinetics of colchicinoid-tubulin associations. *Biochemistry 32*, 2329–2336.
35. Huang, C. Y. (1982) Determination of binding stoichiometry by the continuous variation method. The Job plot. *Methods Enzymol. 87*, 509–525.
36. Ward, L. D. (1985) Measurement of ligand binding to protein by fluorescence spectroscopy. *Methods Enzymol. 117*, 400–414.

37. Bhattacharyya, B., and Wolff, J. (1974) Promotion of fluorescence upon binding of colchicine to tubulin. *Proc. Natl. Acad. Sci. U.S.A. 71*, 2627–2631.
38. Mazumdar, M., Parrack, P. K., Mukhopadhyay, K., and Bhattacharyya, B. (1992) Bis-ANS as a specific inhibitor for microtubule-associated protein induced assembly of tubulin. *Biochemistry 31*, 6740–6744.
39. Horowitz, P., Prasad, V., and Luduena, R. F. (1984) Bis(1,8-anilinonaphthalene-sulfonate): A novel and potent inhibitor of microtubule assembly. *J. Biol. Chem. 259*, 14647–14650.
40. Zhang, B., Liu, J., Pan, J., Han, S., Yin, X., Wang, B., and Hu, G. (2006) Combined treatment with ionizing radiation with genistein on cervical cancer HeLa cells. *J. Pharmacol. Sci. 102*, 129–135.
41. Blajeski, A. L., Phan, V. A., Kottke, T. J., and Kaufmann, S. A. (2002) G1 and G2 cell cycle arrest following microtubule depolymerization in human breast cancer cells. *J. Clin. Invest. 110*, 91–99.
42. Ding, H., Duan, W., Zhu, W.-G., Ju, R., Srinivasan, K., Otterson, G. A., and Villalona-Calero, M. A. (2003) p21 response to DNA damage induced by genistein and etoposide in human lung cancer cells. *Biochem. Biophys. Res. Commun. 305*, 950–956.